Journal of Applied Polymer Science

Template-free Electrochemical Synthesis and Electrochemical Supercapacitors Application of Polyaniline Nanobuds

ShoyebMohamad F. Shaikh,[1,2] Ji-Yeon Lim,[1] Rajaram S. Mane,[3] Manohar K. Zate,[3] Sung-Hwan Han,[4] Oh-Shim Joo[1]

[1]Clean Energy Research Centre, Korea Institute of Science and Technology, Seoul 130-650, Republic of Korea
[2]School of Science, University of Science and Technology, 52 Eoeun dong, Yuseong-gu, Daejeon 305-333, Republic of Korea
[3]Center for Nanomaterials and Energy Devices, School of Physical Science, Swami Ramanand Teerth Marathwada University, Nanded 431606, Maharashtra, India
[4]Inorganic Nanomaterials Laboratory, Department of Chemistry, Hanyang University, Seoul 133-1791, Republic of Korea
Correspondence to: O.-S. Joo (E-mail: joocat@kist.re.kr)

ABSTRACT: One-step and template-free synthesis of polyaniline nanobuds (PANI NBs), synthesized using anodic electrochemical polymerization method, is reported at room temperature onto a conducting indium-tin-oxide glass substrate. The PANI NBs are characterized for their structural, morphological, and electrochromic properties. Scanning electron microscopy image reveals NBs type architecture, perpendicular to the substrate surface. These NBs are broader at their bottoms and narrower at the tops. Individual NB has confirmed 30 nm top diameter and 100–200 nm length. Electrochemical supercapacitive behavior of the PANI NBs electrode is investigated by measuring cyclic voltammetry curves. Moderate specific capacitance of 128 F/g is achieved in the potential range of −0.2 to 1.0 V at 10 mV/s sweep rate in 0.5 *M* H_2SO_4 electrolyte. Influence of inner and outer charges on a resultant specific capacitance is also investigated. © 2012 Wiley Periodicals, Inc. J. Appl. Polym. Sci. 128: 3660–3664, 2013

KEYWORDS: electrochemistry; films; nanoparticles; nanowires; nanocrystals

Received 13 June 2012; accepted 4 September 2012; published online 8 October 2012
DOI: 10.1002/app.38557

INTRODUCTION

Energy storage mechanism in electrochemical supercapacitors (SCs) is interesting on account of their higher energy density than dielectric capacitors and higher power density than batteries.[1] Maintenance-free charging within few seconds, long-term cycling stability, and the ability to deliver up to 10 times power more than batteries are few merits of SCs.[2] Regardless of technology, the main objective of SCs is to develop electrode materials of higher specific capacitance for maximizing energy storage and power at relatively lower electrical resistance. Many academic and industrial laboratories are currently investigating different types of SCs. In general, the electrical double-layer capacitors, based on carbon materials and the pseudocapacitors, related to the redox properties[3] are the two types of SCs. Conducting polymer has been considered in literature as promising candidate for pseudocapacitor electrode materials because of its low cost, facile synthesis, abundant availability, surface interactions, flexibility, and distinctive characteristics of conducting pathways.[4] Many research groups are engaged in increasing the specific power and the specific energy, as well as to produce a long-life device with lower fabrication costs by using environment-friendly materials. Among these, polymer namely polyaniline (PANI) has been considered extensively due to several reasons including tunable high conductivity, low cost, easy synthesis, multiple redox properties, fast response, high capacitive performance, low operating voltage, good environment stability, acid–base properties, and electro chromic behavior, etc.[5] These characteristics operate electrochemical kinetics of redox transitions within the electro-active materials effectively.[6] It is also known that the electrochemical performance is significantly influenced by the surface area and morphology of active materials. The specific capacitance (SC) in PANI is nanostructure-based phenomenon and consequently, a large number of polymerization approaches including self assembly, emulsion, hard and soft-template, interfacial polymerization, seeding, oligomer-assisted[7–9] methods have been proposed, so far, for growing one and three-dimensional forms including nanograins, nanofibers, nanobelts, nanorods, nanowires, nanotubes, hollow microspheres, and ordered whiskers, etc.[10] However, it is noteworthy that the uses of large surfactant and complicated templates have prime importance in all these methods.[11] The high

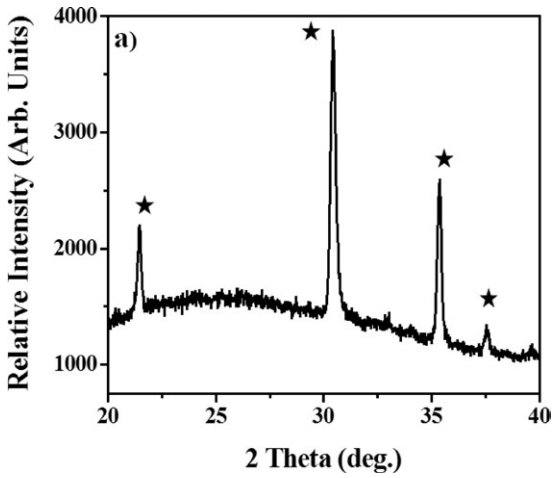

Figure 1. The X-ray diffraction pattern of PANI NBs.

quality of deposition, high through-put, easily tailored 1D nanostructures, low cost and feasibility in controlling growth rate and structural morphologies by simply varying current or potential electrochemical polymerization is in general, the best way to synthesis PANI nanostructures[12] in various forms for envisaging them in portable systems and hybrid electric vehicles, logic circuits, short-term pulses microelectronics, rechargeable batteries, electro-chromic devices, sensors, antistatic coatings, and solar cells, etc.[13,14] A three-step electrochemical route for growing PANI nanowires has been explored by Liu et al.[15] It is reported that the H_2SO_4 concentration increases the rate of hydrolysis under anodic conditions.[16] Using this idea, PANI nanowires arrayed electrodes were successfully grown by means of anodic deposition technique onto Ti/Si substrate using aluminum oxide template.[17] Use of anodic aluminum oxide template is also employed for growing PANI nanostructures.[18] In this work, our aim is to report a unique and simple template-free, one-step and low temperature electrochemical polymerization synthesis method to grow nonaligned NBs of PANI and further employed in structural and morphological measurements. Electrochemical supercapacitor properties are also investigated.

EXPERIMENTAL

Aniline (Qualigens, 99%), in received form, was used as the monomer, which was initially purified by fractional double distillation under reduced pressure. Sulfuric acid (SDFCL, 98%) was used as a dopant, which was used without any further purification. Typically, indium-tin-oxide (ITO) substrates were used as working electrodes. Before the deposition, ITO substrates were ultrasonically cleaned in ultrapure distilled water for 10 min to remove surface contamination and unwanted impurities and then air dried. The electrochemical anodization was carried out from an aqueous solution containing 0.5 *M* aniline and 1 *M* H_2SO_4 at room temperature (300 K).The anodic electrodeposition was performed with three-electrodes in a one-compartment glass cell containing platinum plate (1 × 1 cm^2) as the counter electrode, silver nitrate (Ag/AgCl) as the reference electrode, and ITO (1 × 1 cm^2) as the working electrode. The deposition of PANI NBs was carried out at a constant potential of 0.75 V for 300 s. Above this potential PANI NBs were nonadherent to ITO substrate. The electrochemical polymerization was done through a WonAtech (WPG 100 Potentiostat/Galvanostat Workstation). Subsequent to deposition, the PANI electrode composed of NBs was immersed in 0.1 *M* H_2SO_4 acid and then dried in air and air-baked (annealed) at 60°C for 1 h in order to improve the structural quality, and remove the unwanted impurity if there is any. Mass of the PANI NBs was confirmed from the sensitive nanobalance.

RESULTS AND DISCUSSION

The XRD pattern depicts (Figure 1) reflections, at 2θ values, without any sharp peak and agrees well to previously reported studies,[19] indicating that as-grown PANI NBs were amorphous in nature. The reflection peaks marked with stars revealed the characteristic reflections of ITO, used in the present study as a substrate. To confirm PANI form, energy dispersive X-ray analysis (not shown) measurement was attempted, wherein only carbon and nitrogen elementals were identified. Figure 2 shows the FTIR spectrum of PANI NBs with characteristic bands at 3410, 3321, 3113, 3013, 2881, 1626, 1522, 1378, 1274, 930, 626 and 546 cm^{-1}. Among these, the very weak band at 3410 cm^{-1} was due to the N—H stretching of PANI. The appearance of peaks at 1546 and 1522 cm^{-1} were assigned to the C—C stretching of the quininoid and benzenoid rings, respectively. The band at 1378 cm^{-1} was matched to the emeraldine base structure. Further, the band at 1194 cm^{-1} was caused by an electronic vibration of nitrogen quinine (N—Q—N), where Q represents the quininoid ring.[20] Figure 3(a, b) presents the FE-SEM images of PANI NBs scanned at different magnifications. PANI NBs, which can provide an easy access for ions at the electrode/electrolyte interface for efficient faradic surface reactions, were clearly evidenced. The PANI NBs were about 30 nm in diameters and 200–300 nm in lengths. Homogeneous nucleation and a steric hindrance effect, in general, are two main steps during aniline polymerization process. In homogeneous nucleation, PANI NBs are predominantly formed. However, in the present case, an agglomerated NBs type morphology was obtained. This could be a result of heterogeneous nucleation process as heterogeneous nucleation is, in general,

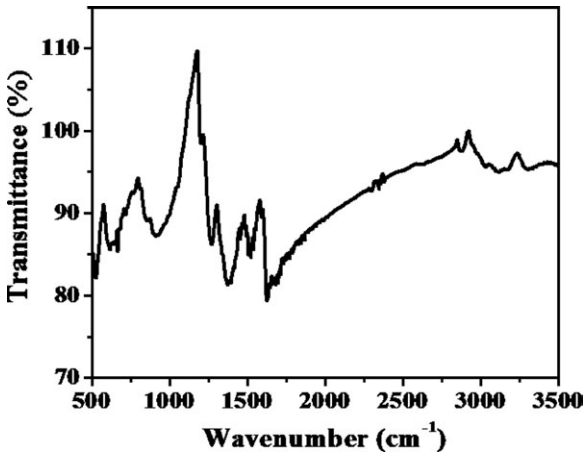

Figure 2. Fourier-transform-infrared measurement spectrum of PANI NBs.

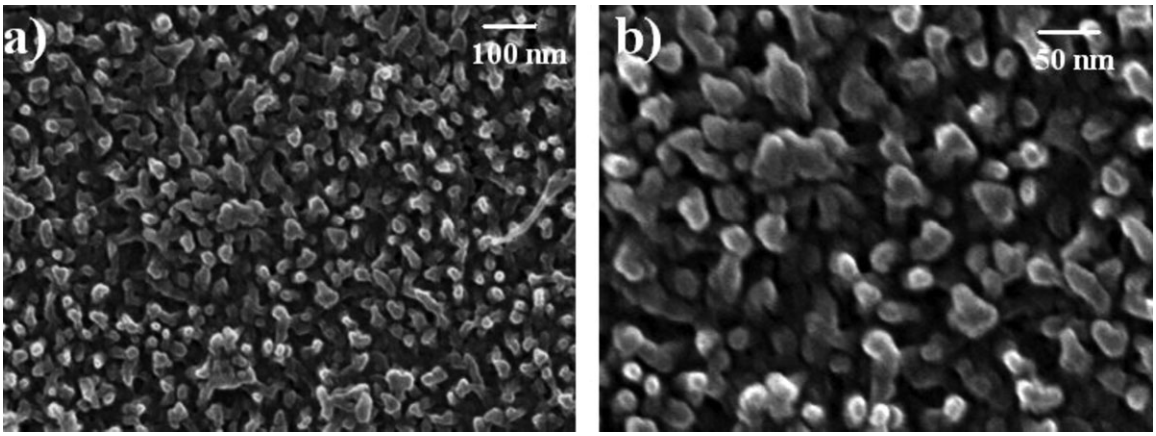

Figure 3. (a, b) FE-SEM images at lower and higher magnifications of the PANI NBs.

a stable phase for critical nucleus formation. According to classical nucleation theory, homogeneous nucleation can be achieved in aqueous solutions by creating sufficiently high levels of super-saturation.[21] As the level of super-saturation increases, both the activation energy and the critical nucleus size decreases. Eventually, as the degree of super-saturation continues to increase, the activation energy becomes so low that results spontaneous and rapid nucleation.[22]

Another significant factor for PANI NBs growth is a steric hindrance effect, which can lead to the formation of NBs with larger diameter at the base and relatively smaller diameter at the top. The homogeneous nucleation might have hindered NBs growth in another way. The redox behavior of PANI depends largely on its form and structure that significantly affects its specific surface area and the ion diffusivity.[23] The cyclic-voltammograms (CVs) of the PANI were recorded at different sweep rates [Figure 4(a)]. The CVs from −0.2 to 1.0 V vs. Ag/AgCl in 0.1 *M* H_2SO_4. The redox reaction of PANI NBs in 0.1 *M* H_2SO_4 was depending on the rate of oxidation of H_2 present in the electrolyte. The CV spectra show asymmetric nature in 0.1 *M* H_2SO_4 proved existence of different redox reactions. The area under the curve was increased with increase in sweep rate, which indicated that the PANI NBs could provide more surfaces for fast reversible faradaic reactions. There were set of redox reaction peaks at higher scan rates, which indirectly demonstrated the high kinetic reversibility of the electrode. As the high sweep rate, the CV curves were deviated from their original shape; the anodic and cathodic peak current densities were relatively similar, indicating that charge and the discharge processes would have occurred reversibly at the electrode/electrolyte interface.[24] The weak peak centered at 0.65 V was due to the oxidation of emeraldine form of PANI, whereas the light peak at 0.86 V was assigned to the pernigraniline form of PANI.[25] The similarity in the shape of the CVs at all scan rates suggested a high efficiency in the capacitive characteristics at the electrode/electrolyte interface. In 0.1 *M* H_2SO_4 relatively better supercapacitor performance was achieved. Figure 4(b) shows the specific capacitance variation against the sweep rate. Specific capacitance of 128 F/g, substantially lower than reported elsewhere[18,26,27] was obtained under at 1mA/cm^2 for 10mV/s sweep rate. Relatively smaller specific capacitance value could be due to presence of hydroxide defect states and week interface interaction between the

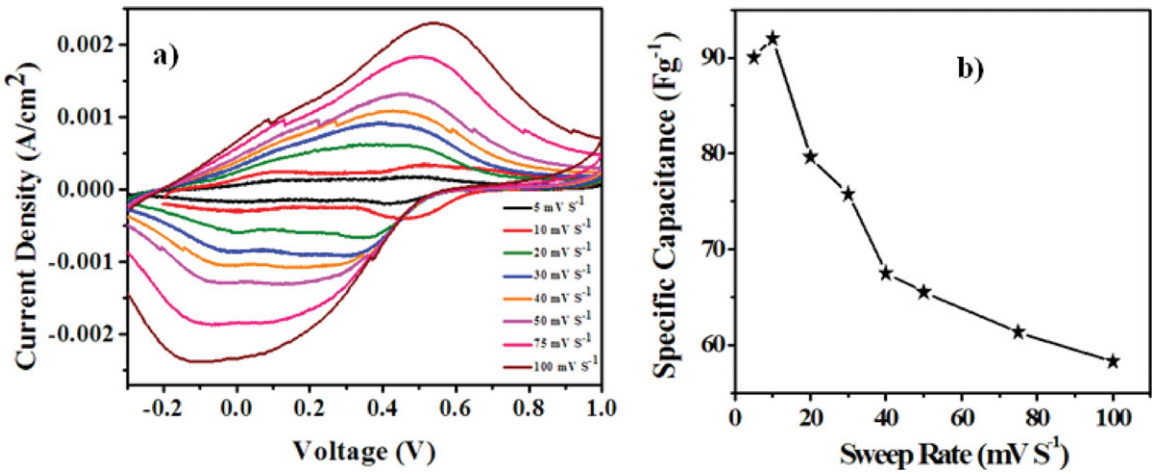

Figure 4. (a) Plots of cyclic-voltammograms versus sweep rate, and (b) specific capacitance versus sweep rate. [Color figure can be viewed in the online issue, which is available at wileyonlinelibrary.com.]

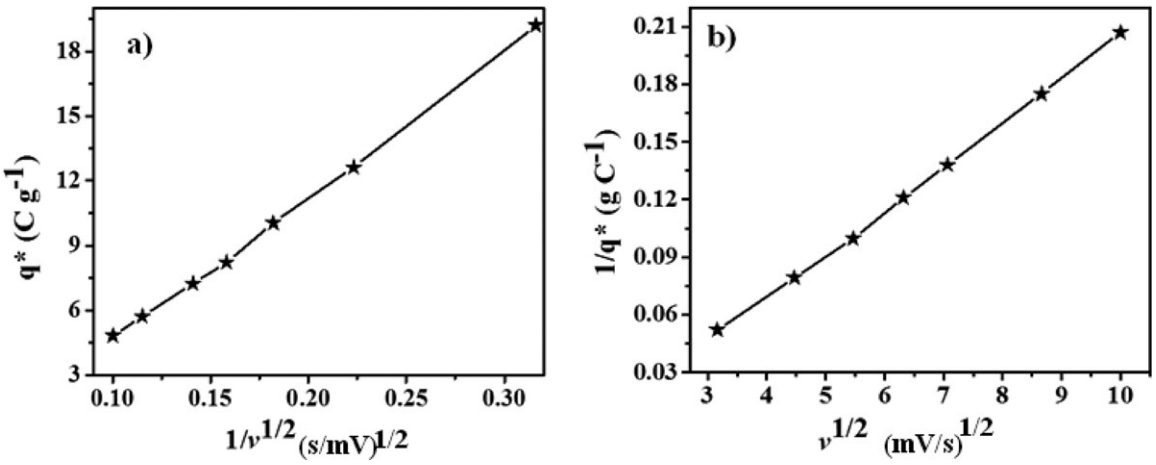

Figure 5. (a) Voltammetric charge q^* versus $1/V^{1/2}$ and (b) $1/q^*$ versus $V^{1/2}$of the PANI NBs.

substrate and the PANI NBs. Low performance at 5 mV/s sweep rate was unprecedented. As the specific capacitance, in general, is directly proportional to sweep rate the voltammetric charges (q^*) were studied as a function of sweep rate which, in particular, is in inversely proportional relation. The dependence of q^* on sweep rate is usually explained by the slow diffusion of protons into pores and grains boundaries. At a high sweep rate, diffusion limitation slows the accessibility of protons to the inner surface of the electrode material, except for more accessible outer surface regions where the diffusion of ions is not hampered.[28] Variation of q^* versus $1/V^{1/2}$ [Figure 5(a)] assuming sweep rate goes to infinite gives outer charge (q^* outer) and variation of $1/q^*$ versus $V^{1/2}$ [Figure 5(b)] assuming sweep rate goes to zero produces total (q^* total) charge. The 28.98 and 2.80 C/cm^2 values were calculated for total and outer charges, respectively. The ratios of inner to total charge (q^* inner/q^* total) and outer to total charge (q^* outer/q^* total) were 0.90 and 0.09, respectively. Presence of higher inner charge was suggesting an easy access of inner species as compared to outer one such that the hydrogen ions can penetrate deep into the PANI NBs matrix for efficient faradic redox reactions.[29] In developing SCs, the electrode material and electrolyte characteristics must be considered jointly. The charge–discharge curves were reversible in nature without apparent deviation in each cycle suggesting that the PANI NBs electrode was of good electrochemical stability.[30] The redox reactions occurred at the electrode/electrolyte interface through faradaic charge-transfer between the electrolyte and the electrode resulted in the enhancement of the specific capacitance. Charging–discharging variations of PANI NBs at constant current density of 1 mA/cm^2 at 10 mV/s were symmetric confirming equal contribution of oxidation and reduction and stable during long-term cycling over 1000 cycles (not shown) revealing that as-grown PANI NBs can be a potential form in optoelectronic devices.

CONCLUSIONS

Amorphous nanobuds of PANI were grown onto conducting ITO substrate using template-free electrochemical method at room temperature and further applied electrochemical SCs application in presence of 0.1 *M* H_2SO_4 as an electrolyte. PANI characteristics bands at various wave numbers confirmed in FTIR spectrum were evidenced the formation of PANI structure. Because of increase in ionic mobility, current density in cyclic-voltammetry was varied with sweep rate. Specific capacitance of 128 F/g (at 10 mV/s) was achieved. This was due to significant inner charge contribution as compared to outer charge.

ACKNOWLEDGMENTS

This work was funded by the, "Hydrogen Energy R&D Center" one of the 21st century frontier R&D programs, funded by Ministry of Science. The authors also acknowledge the research program of the Korea Institute of Science and Technology (KIST). RSM and MKZ wish to thank University Grant Commission, New Delhi, India for providing financial assistance through 41-844/2012(SR) project.

REFERENCES

1. Simon, P.; Gogotsi, Y. *Nat. Mater.* **2008**, *7*, 845.
2. Toupin, M.; Belanger, D.; Hill, I. R.; Quinn, D. *J. Power Source* **2004**, *140*, 203.
3. Wang, Y. G.; Xia, Y. Y. *Electrochim. Acta* **2006**, *51*, 3223.
4. Winter, M.; Brodd, R. *J. Chem. Rev.* **2004**, *104*, 4245.
5. Cui, X. Q.; Li, C. M.; Zang, J. F.; Zhou, Q.; Gan, Y.; Bao, H. F.; Guo, J.; Lee, V. S.; Moochhala, S. M. *J. Phys. Chem. C* **2007**, *111*, 2025.
6. Zhou, Q.; Li, C. M.; Li, J.; Cui, X. Q.; Gervasio, D. *J. Phys. Chem. C* **2007**, *111*, 11216.
7. Li, W.; Wang, H. L. *J. Am. Chem. Soc.* **2004**, *126*, 2278.
8. Virji, S.; Huang, J. X.; Kaner, R. B.; Weiller, B. H. *Nano Lett.* **2004**, *4*, 491.
9. Huang, J.; Kaner, R. B. *Angew. Chem.* **2004**, *116*, 5941.
10. Huang, J.; Kaner, R. B. *J. Am. Chem. Soc.* **2004**, *126*, 851.
11. Werake, L. K.; Story, J. G.; Bertino, M. F.; Pillalamarri, S. K.; Blum, F. D. *Nanotechnology* **2005**, *16*, 2833.
12. Bicelli, L. P.; Bozzini, B.; Mele, C.; Urzo. L. D. *J. Electrochem. Soc.* **2008**, *3*, 356.
13. Zhang, X. Y.; Goux, W. J.; Manohar, S. K. *J. Am. Chem. Soc.* **2004**, *126*, 4502.

14. Terabe, K.; Hasegawa, T.; Nakayama, T.; Aono, M. *Nature* **2005**, *433*, 47.
15. Liu, W.; Cholli, A. L.; Nagarajan, R.; Kumar, J.; Tripathy, S.; Bruno, F. F.; Samuelson, L. *J. Am. Chem. Soc.* **1999**, *121*, 11345.
16. Vivier, V.; Cachet-Vivier, C.; Regis, A.; Sagon, G.; Nedelec, J. Y.; Yu, L. T. *J. Solid State Electrochem.* **2002**, *6*, 522.
17. Hu, C. C.; Chang, H. H.; Lin, M. C.; Wu, Y. T. *Nano Lett.* **2006**, *6*, 2690.
18. Cao, Y.; Mallouk, T. E. *Chem. Mater.* **2008**, *20*, 5260.
19. Yavuz, O.; Ram, M. K.; Aldissi, M.; Poddar, P.; Hariharan, S. *J. Mater. Chem.* **2005**, *15*, 810.
20. Zheng, L.; Wang, Y.; Wang, X.; Li, N.; An, H.; Chen, H.; Guo, J. *J. Power Sources* **2010**, *195*, 1747.
21. Zettlemoyer, A. C., Ed. Nucleation; Marcel Dekker: New York, **1969**.
22. Bunker, B. C.; Rieke, P. C.; Tarasevich, B. J.; Campbell, A. A.; Fryxell, G. E.; Graff, G. L.; Song, L.; Liu, J.; Virden, W. J.; McVay, G. L. *Science* **1994**, *264*, 48.
23. Fusalba, F.; Gouerec, P.; Villers, D.; Belanger, D. *J. Electrochem. Soc.* **2001**, *148*, A1.
24. Nam, K. W.; Yoon, W. S.; Kim, K. B. *Electrochim. Acta* **2002**, *47*, 3201.
25. Stilwell, D. E.; Park, S. M. *J. Electrochem. Soc.* **1988**, *135*, 2491.
26. Li, G. R.; Feng, Z. P.; Zhong, J. H.; Tong, Y.; Wang, Z. L. *Macromolecules* **2010**, *43*, 2178.
27. Dhawale, D. S.; Salunkhe, R. R.; Jamadade, V. S.; Dubal, D. P.; Pawar, S. M.; Lokhande, C. D. *Curr. Appl. Phys.* **2010**, *10*, 904.
28. Sharma, R. K.; Rastogi1, A. C.; Desu, S. B. *Electrochim. Acta* **2008**, *53*, 7690.
29. Soudan, P.; Gaudet, J.; Guay, D.; Bélanger, D.; Schulz, R. *Chem. Mater.* **2002**, *14*, 1210.
30. Chen, Y. M; Cai, J. H.; Huang, Y. S.; Lee, K. Y.; Tsai, D. S. *Nanotechnology* **2011**, *22*, 115706.